ACS Synthetic Biology
Cite This: ACS Synth. Biol. 2018, 7, 1349−1358
Research Article
pubs.acs.org/synthbio

A Green-Light-Responsive System for the Control of Transgene Expression in Mammalian and Plant Cells

Claire Chatelle,[†,‡] Rocio Ochoa-Fernandez,[§,∥,⊥] Raphael Engesser,[‡,#] Nils Schneider,[†,‡] Hannes M. Beyer,[†,‡,§,▽] Alex R. Jones,[○] Jens Timmer,[‡,#] Matias D. Zurbriggen,[*,∥,⊥] and Wilfried Weber[*,†,‡,§]

[†]Faculty of Biology, [‡]BIOSS Centre for Biological Signalling Studies, [§]SGBM Spemann Graduate School of Biology and Medicine, and [#]Institute of Physics, University of Freiburg, Freiburg, 79104, Germany

[∥]Institute of Synthetic Biology, and [⊥]iGRAD Plant Graduate School, Heinrich Heine University, Düsseldorf, 40225, Germany

[○]National Physical Laboratory, Teddington, Middlesex TW11 0LW, U.K.

Supporting Information

ABSTRACT: The ever-increasing complexity of synthetic gene networks and applications of synthetic biology requires precise and orthogonal gene expression systems. Of particular interest are systems responsive to light as they enable the control of gene expression dynamics with unprecedented resolution in space and time. While broadly used in mammalian backgrounds, however, optogenetic approaches in plant cells are still limited due to interference of the activating light with endogenous photoreceptors. Here, we describe the development of the first synthetic light-responsive system for the targeted control of gene expression in mammalian and plant cells that responds to the green range of the light spectrum in which plant photoreceptors have minimal activity. We first engineered a system based on the light-sensitive bacterial transcription factor CarH and its cognate DNA operator sequence CarO from *Thermus thermophilus* to control gene expression in mammalian cells. The system was functional in various mammalian cell lines, showing high induction (up to 350-fold) along with low leakiness, as well as high reversibility. We quantitatively described the systems characteristics by the development and experimental validation of a mathematical model. Finally, we transferred the system into *A. thaliana* protoplasts and demonstrated gene repression in response to green light. We expect that this system will provide new opportunities in applications based on synthetic gene networks and will open up perspectives for optogenetic studies in mammalian and plant cells.

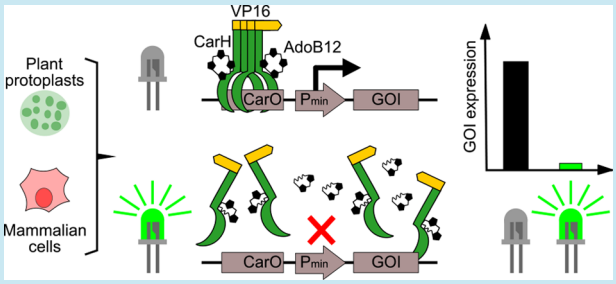

KEYWORDS: *optogenetics, light-responsive gene expression, green light, CarH, AdoB12, plants*

Inducible gene switches are core innovations in synthetic biology that enable the programming of cellular function.[1,2] Such programming has provided novel opportunities in functional genomics[3] as well as in drug discovery[4] but has also enabled the implementation of smart biomaterials[5] or the design of closed loop-controlled gene and cell therapeutic networks.[6,7] Inducible gene expression technology in mammalian cells was pioneered by antibiotic-responsive gene switches[8−10] and has rapidly expanded in the inducer spectrum. Gene activity can now be controlled in response to different drugs, metabolites, quorum-sensing messengers or, more recently, in response to light of a specific wavelength.[11−14] Light as inducer offers control opportunities with unmatched resolution in space and time. Such optogenetic switches are based on wiring plant- or bacteria-derived photoreceptors to genetic control elements to activate or repress transcription in animal cells in response to UVB, blue, red or far-red light (www.optobase.org).[13] While such control is now routine in mammalian cells, the application of optogenetic strategies in plant cells lags behind[15] as it is still limited by the endogenous plant photoreceptors that would be cross-activated by the inducing light and thereby might yield off-target signaling responses.[16,17] One opportunity to foster the potential of optogenetics in plants, however, would be the design of a green light-responsive gene switch, as plant photoreceptors show reduced activity in this part of the light spectrum.[18] In this work, we describe the development and characterization of the first green-light-responsive gene switch in mammalian and plant cells. This work extends the toolbox for optogenetic control in mammalian cells and opens opportunities for targeted genetic interventions in plant cell backgrounds. The system is inspired by a naturally occurring defense mechanism found in Gram-negative bacteria such as *Myxococcus xanthus* and *Thermus thermophilus* to protect themselves against photo-oxidative stress.[19−21] In those organisms, CarH, a light-responsive

Received: December 12, 2017
Published: April 10, 2018

DOI: 10.1021/acssynbio.7b00450
ACS Synth. Biol. 2018, 7, 1349−1358

transcription factor, regulates the expression of a carotenogenic gene cluster. CarH activity and light-sensitivity is dependent on the coenzyme, 5′deoxyadenosylcobalamin (AdoB12). In darkness, AdoB12-linked CarH binds to the DNA operator CarO as a tetramer leading to repression of the carotenogenic target genes. Upon illumination, the Co−C bond in AdoB12 is disrupted by photolysis,[22] which triggers disassembly and release of the tetramer from CarO thus derepressing gene expression.[22,23] Recently, a light-responsive fibroblast growth factor receptor[24] (FGFR) and a light-tunable polymer matrix[25] based on this light-inducible CarH dissociation have been constructed. As AdoB12 features an absorption peak in the green region of the light spectrum (525 nm),[26] we hypothesized that the system could be used for the implementation of a green-light-responsive gene expression system. We engineered the light-responsive CarH-CarO interaction to control gene expression in different mammalian cell lines. We quantitatively characterized the performance of the system by the development and parametrization of a mathematical model. We finally demonstrated the utility of the system for light-regulated gene expression in plant protoplasts.

The green light-responsive gene expression system in mammalian cells consists of two constructs (Figure 1a). The

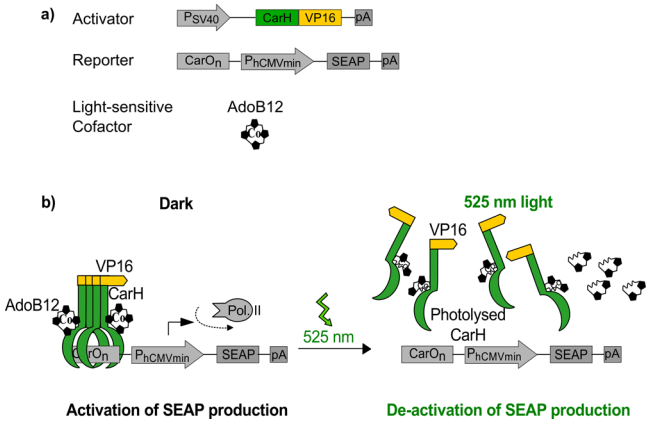

Figure 1. Design of the green-light-responsive gene expression system. (a) Molecular components of the expression system. The activator plasmid encodes the DNA binding protein CarH fused to the *Herpes simplex* transactivation domain VP16 under the control of the constitutive simian virus 40 promoter (P_{SV40}). The reporter plasmid is composed of multimeric CarO sequences upstream of a human cytomegalovirus-derived minimal promoter ($P_{hCMVmin}$) controlling expression of secreted alkaline phosphatase (SEAP). The light-sensitivity of the system is conferred by the chromophore AdoB12. (b) Mode of function. In the dark, CarH-VP16 bound to AdoB12 forms tetramers that bind CarO thereby recruiting RNA polymerase II (Pol II) and activating SEAP expression. Exposure to green light leads to photolysis of AdoB12 what triggers destabilization of CarH tetramers and the release of CarO thereby deactivating SEAP expression.

first one encodes the CarH protein fused to the *Herpes simplex* virus-derived VP16 transactivation domain[27] to be expressed under the control of the constitutive simian virus 40 promoter (P_{SV40}). The second one is a reporter plasmid composed of a multimeric CarO sequence upstream of the minimal human cytomegalovirus promoter sequence ($P_{hCMVmin}$) controlling the expression of a gene of interest, here the secreted alkaline phosphatase (SEAP) reporter gene. Transfection of the constructs into mammalian cells, followed by supplementation with AdoB12 in the dark, leads to the formation of CarH-VP16 tetramers binding to the CarO sequence. VP16 will recruit the transcription initiation complex to start RNA polymerase II-dependent SEAP expression (Figure 1b). However, upon green light exposure, CarH-VP16 tetramers dissociate and release CarO, which terminates SEAP expression (Figure 1b). Although only produced by microorganisms, AdoB12 is essential for many metabolic processes in mammals and hence, mammalian cells are capable of both AdoB12 import and conversion of biologically inactive forms of B12 into AdoB12.[28,29]

To analyze the functionality of the system in mammalian cells, a first proof-of-principle experiment was performed using the activator CarH-VP16 and the reporter $CarO_2$, containing two consecutive repeat sequences of the DNA operator, upstream of the minimal promoter mediating SEAP expression. The light insensitive E-OFF system,[30] consisting of the activator E-VP16 binding to the DNA operator ETR, upstream of a minimal promoter mediating SEAP expression, was used as control to analyze possible effects of AdoB12 and green light on gene expression. Human embryonic kidney 293 (HEK-293) cells were transfected with the corresponding activator and reporter plasmids. Twenty-four hours post-transfection the culture medium was supplemented (when indicated) with 10 μM AdoB12. Cells were kept in the dark or exposed to green (525 nm) light (5 μmol m^{-2} s^{-1}) for another 24 h, before measuring SEAP production (Figure 2). Cells transfected with

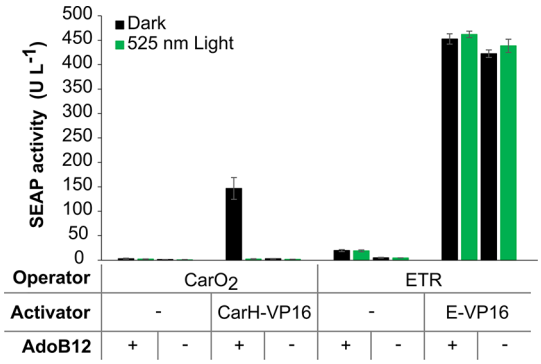

Figure 2. Proof of principle experiment showing the functionality of the green light-responsive gene expression system in mammalian cells. HEK-293 cells were transfected with reporter ($CarO_2$, pCVC034; ETR, pWW37) and activator (CarH-VP16, pHB144; E-VP16, pWW35) plasmids as indicated. After 24 h cells were supplemented with 10 μM AdoB12 where indicated (+) and either kept in dark (black bars) or exposed to 525 nm light (5 μmol m^{-2} s^{-1}, green bars) for another 24 h. SEAP production was determined from cell culture supernatants. Data are means ± Stdev (n = 3).

the ETR reporter plasmid only expressed SEAP in the presence of the corresponding activator E-VP16. Neither the addition of AdoB12 nor illumination resulted in significantly changed SEAP production. Cells transfected with the $CarO_2$ reporter plasmid only expressed SEAP in the presence of CarH-VP16 upon supplementation with AdoB12 and cultivation in the dark. Exposure to green light, however, reduced SEAP production 73-fold to levels observed in negative controls (without CarH-VP16).

However, maximum SEAP production levels of the CarH-based system (147 U L^{-1}) were still lower than the ones obtained using the well-established E-system (450 U L^{-1}), which prompted us to evaluate different optimization strategies.

DOI: 10.1021/acssynbio.7b00450
ACS Synth. Biol. 2018, 7, 1349−1358

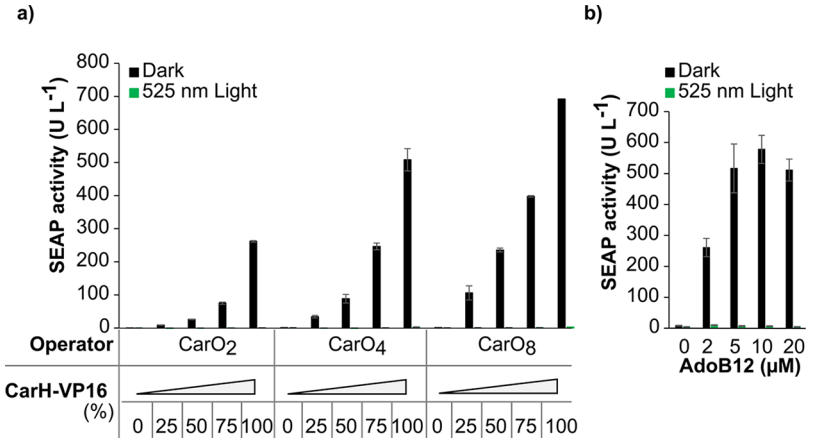

Figure 3. Optimization of the green-light-responsive gene expression system. (a) Impact of the number of CarO repeats and the CarH/CarH-VP16 ratio on SEAP activity. HEK-293 cells were transfected with reporter plasmids containing an increasing number of CarO repeats ($CarO_2$, pCVC034; $CarO_4$, pCVC035; $CarO_8$, pCVC036) and with different amounts of expression plasmids for CarH-VP16 (pHB144, indicated in %) completed to 100% with plasmid pCVC025 for expression of CarH. After 24 h cells were supplemented with 10 μM AdoB12 and either kept in the dark (black bars) or exposed to 525 nm light (5 μmol m^{-2} s^{-1}, green bars) for another 24 h. SEAP activity was determined from cell culture supernatants. (b) Impact of AdoB12 concentration on SEAP activity. HEK-293 cells were transfected with plasmids pCVC036 ($CarO_8$) and pHB144 (CarH-VP16). After 24 h, the concentrations of AdoB12 indicated were added followed by 24 h cultivation in the dark or under 525 nm light prior to measurement of SEAP activity. Data are means ± Stdev (n = 3).

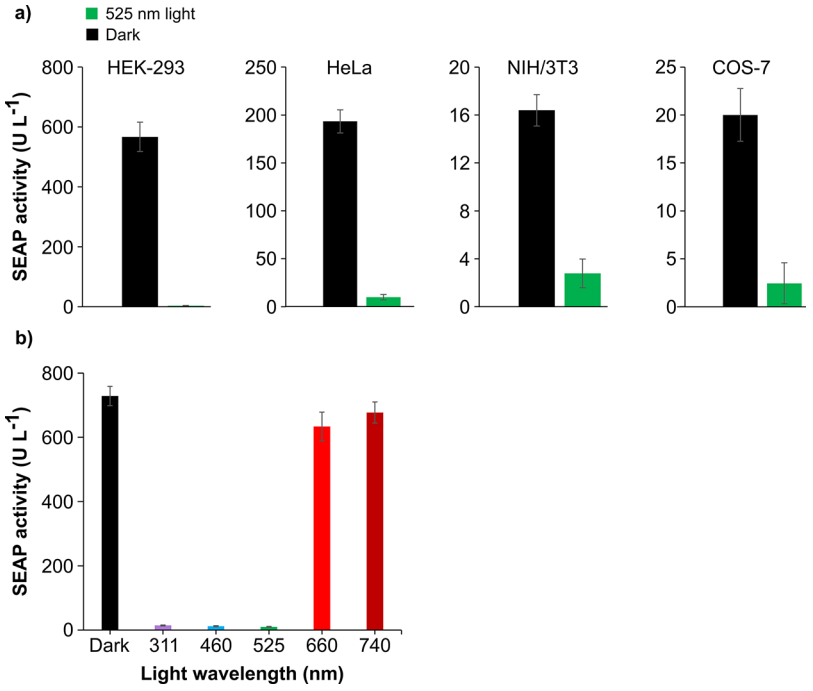

Figure 4. Characterization of the green light-responsive expression system in different mammalian cell lines and for different illumination wavelengths. (a) Human embryonic kidney cells (HEK-293), human cervix carcinoma cells (HeLa), mouse fibroblasts (NIH/3T3), and African green monkey kidney fibroblast-like cells (COS-7) were transfected with plasmids pCVC036 ($CarO_8$) and pHB144 (CarH-VP16). After 24 h cells were supplemented with 10 μM AdoB12 and either kept in dark (black bars) or exposed to 525 nm light (green bars). After 24 h, SEAP activity was determined. (b) Response to light of different wavelengths. The following illumination regimes were used: UVB (cycles of pulsed 311 nm light, 0.8 μmol m^{-2} s^{-1} for 2 min followed by 48 min dark); blue light (460 nm, 4 μmol m^{-2} s^{-1}); green light (525 nm, 5 μmol m^{-2} s^{-1}); red light (660 nm, 8 μmol m^{-2} s^{-1}); far-red light (740 nm, 80 μmol m^{-2} s^{-1}). Data are means ± Stdev (n = 3).

The system involves three main components: CarH-VP16, CarO and AdoB12. Any of these components could be modified/adjusted to optimize gene induction characteristics. We hypothesized that the fusion to VP16 might impact CarH activity and that the addition of wild type CarH might overcome such issues, for example, by the formation of heterotetramers. To analyze this possibility, we supplemented CarH-VP16 with wild type CarH, in different ratios. The results, however, revealed that SEAP activity was maximal in cells transfected with 100% CarH-VP16, indicating that free CarH did not have beneficial effects on gene expression characteristics (Figure 3a). Next, in order to determine an optimized promoter configuration we varied the number of CarO sequences in the reporter plasmid. The experiments

DOI: 10.1021/acssynbio.7b00450
ACS Synth. Biol. 2018, 7, 1349−1358

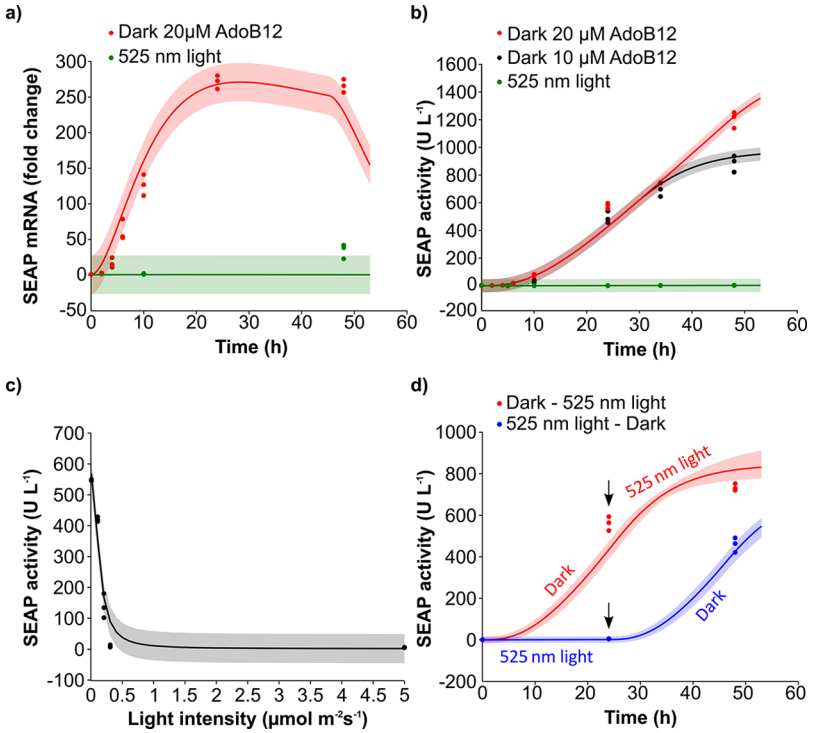

Figure 5. Quantitative characterization of the green-light-responsive expression system. In all experiments HEK-293 cells were transfected with plasmids pCVC036 ($CarO_8$) and pHB144 (CarH-VP16). After 24 h cells were supplemented with the indicated concentrations of AdoB12 and cultivated for another 48 h using the indicated illumination schemes prior to determining SEAP mRNA or protein production. (a) Time course of SEAP mRNA production. (b) Time course of SEAP protein production. (c) Impact of different light intensities on gene expression. 525 nm light was used at the indicated intensities and SEAP production was quantified after 24 h. In panels a–c the points represent individual data values from triplicate measurements. The curves represent the model fit to the data, and the shaded error bands are estimated by an error model with a constant Gaussian error. (d) Validation of the model predictions. Model-based prediction of SEAP production kinetics for the indicated illumination schemes (assuming 20 μM AdoB12 addition at $t = 0$). The shaded bands indicate the 95% prediction confidence interval. The black arrows indicate the change in illumination conditions. The data points represent results from triplicate validation experiments using the indicated experimental conditions.

revealed that increasing the number of operator sequences, and thus of binding sites for CarH-VP16, led to a higher activation of the system, reflected by an increased SEAP production (Figure 3a). Doubling the number of operator sites from two to four resulted in a 2-fold increase in SEAP production; adding another four CarO operators resulted in a further 1.4-fold increased SEAP production. Finally, we analyzed the impact of AdoB12 concentration. We found that 10 μM AdoB12 were sufficient for complete activation of the system (Figure 3b). To conclude, the optimized system consists of a reporter plasmid containing an octameric $CarO_8$ operator, the light-regulated activator CarH-VP16, and supplementation of the cell culture medium with 10 μM AdoB12. In HEK-293 cells, this configuration showed to be very tightly repressed under green light and could be induced by up to 350-fold in darkness. These experimental conditions were used throughout the subsequent experiments. We next evaluated the suitability of the system for green light-responsive gene expression in different human-, mouse- and monkey-derived cell lines. We observed high induction levels, suggesting cross-species applicability of this expression control strategy (Figure 4a). However, there were differences in absolute SEAP production values. Such cell line-dependent differences are commonly observed with inducible expression systems and can be attributed to several cell-dependent factors, such as transfection efficiency, cell line-specific promoter strength or interference with endogenous signaling pathways.[30−33] Next, we analyzed the responsiveness of the CarH system to illumination wavelengths and intensities commonly used in other optogenetic systems.[34] To this end, we evaluated SEAP production in response to UVB (311 nm), blue (460 nm), red (660 nm), and far-red (740 nm) light. Whereas illumination in the red spectrum did not affect CarH-dependent gene expression, blue and UVB light reduced SEAP production (Figure 4b). This cross-reactivity can be explained by the photolysis of AdoB12 also at shorter wavelengths.[22] These data further demonstrate that the CarH system could be used in combination with red light-responsive optogenetic systems[33,35,36] for the orthogonal control of cellular processes and that red light can be used as safe light when handling the system.

To enable predictable and reliable application of green light-responsive gene expression, we next performed a detailed quantitative characterization of the system's performance. To characterize the early stages of reporter expression, we quantified mRNA expression levels with RT-qPCR in the presence of 20 μM AdoB12 for 48 h (Figure 5a). In the dark and after an initial lag-phase of approximately 1 h, SEAP mRNA levels increased rapidly and reached a maximum of approximately 270-fold induction after 24 h and stagnated afterward. In parallel, we determined SEAP protein production kinetics in the dark and under green light (Figure 5b). While gene expression remained at background levels under 525 nm light, cultivation in the dark resulted in continuously increasing SEAP levels. We further hypothesized, that one limiting factor of the

DOI: 10.1021/acssynbio.7b00450
ACS Synth. Biol. 2018, 7, 1349−1358

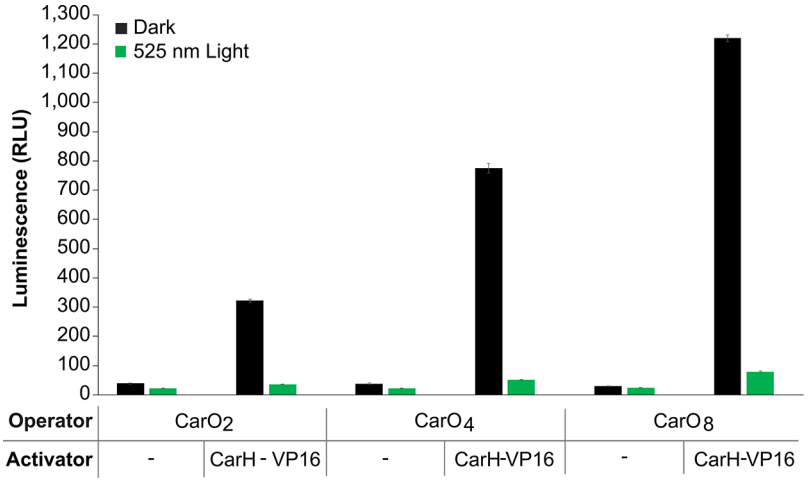

Figure 6. Characterization of the green light-responsive expression system in *A. thaliana* protoplasts. Reporter plasmids with increasing number of CarO repeats ($CarO_2$, pROF250; $CarO_4$, pROF251; $CarO_8$, pROF252) were transformed in a 3:1 molar ratio over the CarH-VP16 expression plasmid pROF254. After transformation, protoplasts were supplemented with AdoB12 to a final concentration of 20 μM. After cultivation in the dark or under 525 nm light (5 μmol m^{-2} s^{-1}) luciferase activity was determined. Data are means ± SEM (n = 6). RLU: relative luminescence units.

system could be the availability of AdoB12. Indeed, while SEAP protein production in the presence of 10 μM AdoB12 showed comparable early stage dynamics as for 20 μM, the SEAP production rate declined after approximately 30 h. This decline can be attributed to AdoB12 degradation as time-course experiments revealed a half-life time for AdoB12 of 22.6 ± 4.9 h in a cell culture environment (Supplementary Figure 1). This suggests that higher initial AdoB12 concentrations or a resupplementation of the cofactor would be required for longer experiments. Next, we analyzed the adjustability of the system in response to increasing light intensities (Figure 5c). Maximum expression levels were reached in the dark, whereas very low light intensities (0.1−0.3 μmol m^{-2} s^{-1} corresponding to 2.3−6.8 μW cm^{-2}) resulted in intermediate expression values. At light intensities of 5 μmol m^{-2} s^{-1} gene expression was in the low off state.

To obtain quantitative insight into the systems characteristics, we developed a mathematical model and inferred kinetic parameters from the experiments described above (Figure 5a,b,c and Supplementary Figure 1). We based the model on the following ordinary differential equations:

$$\frac{\mathrm{d}[\mathrm{AdoB12}](t)}{\mathrm{d}t} = -Nk_{\mathrm{deg,B12}}[\mathrm{AdoB12}] - k_{\mathrm{form,CarH\_B12}}[\mathrm{CarH}][\mathrm{AdoB12}] \quad (1)$$

$$\frac{\mathrm{d}[\mathrm{CarH}](t)}{\mathrm{d}t} = GDk_{\mathrm{prod,CarH}} - k_{\mathrm{deg,CarH}}[\mathrm{CarH}] - k_{\mathrm{form,CarH\_B12}}[\mathrm{CarH}][\mathrm{AdoB12}] \quad (2)$$

$$\frac{\mathrm{d}[\mathrm{CarH\_B12}](t)}{\mathrm{d}t} = -k_{\mathrm{deg,CarH}}[\mathrm{CarH\_B12}] + k_{\mathrm{form,CarH\_B12}}[\mathrm{CarH}][\mathrm{B12}] - k_{\mathrm{off}}I(t)[\mathrm{CarH\_B12}] \quad (3)$$

$$\frac{\mathrm{d}[\mathrm{CarH\_B12_{off}}](t)}{\mathrm{d}t} = k_{\mathrm{off}}I(t)[\mathrm{CarH\_B12}] \quad (4)$$

$$\frac{\mathrm{d}[\mathrm{mRNA1}](t)}{\mathrm{d}t} = GD\left(k_{\mathrm{basal,mRNA}} + k_{\mathrm{tc,mRNA}}\frac{[\mathrm{CarH\_B12}]^2}{K_{\mathrm{m,tc}}^2 + [\mathrm{CarH\_B12}]^2}\right) - k_{\mathrm{process,mRNA}}[\mathrm{mRNA1}] \quad (5)$$

$$\frac{\mathrm{d}[\mathrm{mRNA2}](t)}{\mathrm{d}t} = k_{\mathrm{process,mRNA}}[\mathrm{mRNA1}] - k_{\mathrm{deg,mRNA}}[\mathrm{mRNA2}] \quad (6)$$

$$\frac{\mathrm{d}[\mathrm{SEAP}](t)}{\mathrm{d}t} = k_{\mathrm{tl,SEAP}}[\mathrm{mRNA2}]N \quad (7)$$

$$\frac{\mathrm{d}N(t)}{\mathrm{d}t} = k_{\mathrm{growth}}N\left(1 - \frac{N}{N_{\mathrm{max}}}\right) \quad (8)$$

with

$$\mathrm{GD} = \frac{1}{N}$$

The model describes the temporal evolution of the concentrations of the relevant molecules. The first three equations capture the dynamics of AdoB12 and CarH-VP16 (denoted as CarH). AdoB12 degrades linearly and binds with CarH-VP16 to the CarH-VP16_AdoB12 complex (denoted as CarH_B12). CarH-VP16 is produced at a constant rate by the constitutive promoter P_{SV40} and degraded by first order kinetics. It is further inactivated by 525 nm light at a rate proportional to the light intensity, $I(t)$. The production of the target mRNA is induced by the active CarH-VP16_AdoB12 complex with a Hill-function. To represent transcription and mRNA transport out of the nucleus, mRNA synthesis is modeled in two steps. The resulting mRNA is degraded linearly and translated into the SEAP protein at the rate $k_{\mathrm{tl,SEAP}}$. The growth of cell number (N) is described by a logistic growth curve with the specific growth rate k_{growth} and the maximal cell count N_{max}. Plasmid dilution in transient transfections is covered by the factor gene dose (GD), which is inversely proportional to the number of cells. A detailed description and derivation of the mathematical model is presented in the Supporting Information. The unknown model parameters were estimated from experimental data by utilizing a maximum likelihood approach, which follows the strategy described by Müller *et al.*[34] For the calibration, we used the time course data shown in Figure 5a (SEAP mRNA time course) and Figure 5b (SEAP protein time course), the light dose−response data depicted in Figure 5c, AdoB12 dose−response data (Supplementary Figure 1a), as well as stability measurements of AdoB12 (Supplementary Figure 1b). The measuring error (shaded bands) was captured by an error model with a constant Gaussian error that was estimated simultaneously with the dynamical parameters. To assess the uncertainty of the estimated parameter in terms of their 95%

DOI: 10.1021/acssynbio.7b00450
ACS Synth. Biol. 2018, 7, 1349−1358

Table 1. Vectors Used in This Study

Plasmid	Description	Reference
pHB144	P_{SV40}-CarH-VP16-pA DNA sequence for CarH-VP16 (CarH, italics; VP16, underlined) *ATGACCTCCTCCGGGGTGTACACCATCGCCGAGGTGGAAGCCATGACCGGC* *CTTTCCGCCGAGGTGCTCCGCCAGTGGGAGCGCCGCTACGGCTTCCCCAAG* *CCCCGGCGTACCCCGGGAGGGCATCGCCTCTACAGCGCGGAAGACGTGGA* *GGCCCTGAAGACGATCAAGCGCTGGCTGGAGGAGGGGGCCACGCCTAAAG* *CGGCCATCCGCCGCTACCTGGCCCAGGAGGTGCGCCCCGAGGACCTGGGG* *ACCGGCCTCCTCGAGGCCCTCCTCCGGGGGGACCTCGCCGGGGCCGAGGC* *CCTCTTCCGCCGGGGGCTCAGGTTTTGGGGCCCGGAGGGCGTCCTGGAGC* *ACCTCCTCCTCCCCGTCCTCCGGGAGGTGGGGGAGGCCTGGCACCGGGGG* *GAGATCGGGGTGGCGGAGGAGCACCTGGCCTCCACCTTCCTCCGGGCAAG* *GCTCCAGGAACTTTTGGACCTCGCGGGCTTCCCGCCCGGGCCCCCCGTCCT* *CGTCACCACCCCTCCCGGGGAGCGGCACGAGATCGGGGCCATGCTCGCCG* *CCTACCACCTCCGCCGCAAAGGGGTCCCCGCCCTCTACCTCGGCCCCGACA* *CACCTCTCCCCGACCTCAGGGCCTTGGCCCGGCGGCTCGGGGCGGGGGCG* *GTGGTCCTCTCCGCCGTCCTTTCCGAGCCTTTAAGGGCCCTCCCCGACGGG* *GCCCTTAAGGACCTCGCCCCCCGGGTCTTCCTCGGGGGGCAGGGGGCGGG* *GCCGGAGGAGGCCAGGAGGCTCGGCGCCGAGTACATGGAGGACCTGAAGG* *GCCTCGCCGAGGCCCTTTGGCTCCCTAGGGGGCCGGAAAAGGAGGCGATA* GGCGCCGGCGCCGGCGCGCGTACGAAAAACAATTACGGGTCTACCATCGAG GGCCTGCTCGATCTCCCGGACGACGACGCCCCCGAAGAGGCGGGGCTGGC GGCTCCGCGCCTGTCCTTTCTCCCCGCGGGACACACGCGCAGACTGTCGAC GGCCCCCCCGACCGATGTCAGCCTGGGGGACGAGCTCCACTTAGACGGCG AGGACGTGGCGATGGCGCATGCCGACGCGCTAGACGATTTCGATCTGGACA TGTTGGGGGACGGGGATTCCCCGGGTCCGGGATTTACCCCCCACGACTCCG CCCCCTACGGCGCTCTGGATATGGCCGACTTCGAGTTTGAGCAGATGTTTAC CGATGCCCTTGGAATTGACGAGTACGGTGGGTAG	This work
pCVC025	P_{CMV}-CarH-pA DNA sequence for CarH ATGACCTCCTCCGGGGTGTACACCATCGCCGAGGTGGAAGCCATGACCGGC CTTTCCGCCGAGGTGCTCCGCCAGTGGGAGCGCCGCTACGGCTTCCCCAAG CCCCGGCGTACCCCGGGAGGGCATCGCCTCTACAGCGCGGAAGACGTGGA GGCCCTGAAGACGATCAAGCGCTGGCTGGAGGAGGGGGCCACGCCTAAAG CGGCCATCCGCCGCTACCTGGCCCAGGAGGTGCGCCCCGAGGACCTGGGG ACCGGCCTCCTCGAGGCCCTCCTCCGGGGGGACCTCGCCGGGGCCGAGGC CCTCTTCCGCCGGGGGCTCAGGTTTTGGGGCCCGGAGGGCGTCCTGGAGC ACCTCCTCCTCCCCGTCCTCCGGGAGGTGGGGGAGGCCTGGCACCGGGGG GAGATCGGGGTGGCGGAGGAGCACCTGGCCTCCACCTTCCTCCGGGCAAG GCTCCAGGAACTTTTGGACCTCGCGGGCTTCCCGCCCGGGCCCCCCGTCCT CGTCACCACCCCTCCCGGGGAGCGGCACGAGATCGGGGCCATGCTCGCCG CCTACCACCTCCGCCGCAAAGGGGTCCCCGCCCTCTACCTCGGCCCCGACA CACCTCTCCCCGACCTCAGGGCCTTGGCCCGGCGGCTCGGGGCGGGGGCG GTGGTCCTCTCCGCCGTCCTTTCCGAGCCTTTAAGGGCCCTCCCCGACGGG GCCCTTAAGGACCTCGCCCCCCGGGTCTTCCTCGGGGGGCAGGGGGCGGG GCCGGAGGAGGCCAGGAGGCTCGGCGCCGAGTACATGGAGGACCTGAAGG GCCTCGCCGAGGCCCTTTGGCTCCCTAGGGGGCCGGAAAAGGAGGCGATAT AG	This work
pCVC034	$CarO_2$-$P_{hCMVmin}$-SEAP-pA DNA sequence (5'->3') of $CarO_2$-$P_{hCMVmin}$ (CarO, italics; $P_{hCMVmin}$, underlined) *ACACTCCGCAGAGATGTACAAAAGCTTGACAAAAACCTA*GCTAGA*ACACTCC* *GCAGAGATGTACAAAAGCTTGACAAAAACCTA*GCTAGCGATATCATCGCCGG TACCTGATATATAGTTAGGCGTGTACGGTGGGAGGCCTATATAAGCAGAGCT CGTTTAGTGAACCGTCAGATCGCCTGGAGACGCCATCCACGCTGTTTTGACC TCCATAGAAGACACCGGGACCGATCCAGCCT	This work
pCVC035	$CarO_4$-$P_{hCMVmin}$-SEAP-pA DNA sequence (5'->3') of $CarO_4$-$P_{hCMVmin}$ (CarO, italics; $P_{hCMVmin}$, underlined) *ACACTCCGCAGAGATGTACAAAAGCTTGACAAAAACCTA*GCTAGA*ACACTCC* *GCAGAGATGTACAAAAGCTTGACAAAAACCTA*GCTAGA*ACACTCCGCAGAGA* *TGTACAAAAGCTTGACAAAAACCTA*GCTAGA*ACACTCCGCAGAGATGTACAAA* *AGCTTGACAAAAACCTA*GCTAGCGATATCATCGCCGGTACCTGATATATAGTT AGGCGTGTACGGTGGGAGGCCTATATAAGCAGAGCTCGTTTAGTGAACCGTC AGATCGCCTGGAGACGCCATCCACGCTGTTTTGACCTCCATAGAAGACACCG GGACCGATCCAGCCT	This work

DOI: 10.1021/acssynbio.7b00450
ACS Synth. Biol. 2018, 7, 1349−1358

Table 1. continued

Plasmid	Description	Reference
pCVC036	$CarO_8$-$P_{hCMVmin}$-SEAP-pA DNA sequence (5'->3') of $CarO_8$-$P_{hCMVmin}$ (CarO, italics; $P_{hCMVmin}$, underlined) *ACACTCCGCAGAGATGTACAAAAGCTTGACAAAAACCTA*GCTAGAACACTCC *GCAGAGATGTACAAAAGCTTGACAAAAACCTA*GCTAGAACACTCCGCAGAGA *TGTACAAAAGCTTGACAAAAACCTA*GCTAGAACACTCCGCAGAGATGTACAAA *AGCTTGACAAAAACCTA*GCTAGAACACTCCGCAGAGATGTACAAAAGCTTGA *CAAAAACCTA*GCTAGAACACTCCGCAGAGATGTACAAAAGCTTGACAAAAAC *CTA*GCTAGAACACTCCGCAGAGATGTACAAAAGCTTGACAAAAACCTAGCTA *GAACACTCCGCAGAGATGTACAAAAGCTTGACAAAAACCTA*GCTAGCGATAT CATCGCCGGTACCTGATATATAGTTAGGCGTGTACGGTGGGAGGCCTATATA AGCAGAGCTCGTTTAGTGAACCGTCAGATCGCCTGGAGACGCCATCCACGCT GTTTTGACCTCCATAGAAGACACCGGGACCGATCCAGCCT	This work
pROF250	$CarO_2$-$P_{hCMVmin}$-Luciferase-pA	This work
pROF251	$CarO_4$-$P_{hCMVmin}$-Luciferase-pA	This work
pROF252	$CarO_8$-$P_{hCMVmin}$-Luciferase-pA	This work
pROF254	$P_{CaMV35s}$-CarH-VP16-pA	This work
pWW35	P_{SV40}-E-VP16-pA	30
pWW37	ETR-$P_{hCMVmin}$-SEAP-pA	30

confidence intervals the parameter profile likelihood was evaluated.[37] The analysis was performed with the Data2-Dynamics framework[38] (see Supporting Information for details on the parameter estimation and uncertainty analysis).

We finally analyzed whether the model can be applied to predict gene expression profiles as a function of the illumination regime. We simulated SEAP production profiles in the dark ($I(t) = 0$) and under green light ($I(t) = 5$ μmol m^{-2} s^{-1}), and when swapping the illumination conditions after 24 h. The model prediction revealed a high reversibility of the system: after 24 h illumination under 525 nm light no significant activation was expected, whereas transferring the system to the dark initiated SEAP production (Figure 5d, blue curve). On the other hand, turning on the green light after 24 h stopped SEAP production (Figure 5d, red curve). The prediction uncertainties in terms of their 95% confidence intervals (Figure 5d) were inferred by propagating the uncertainty of the estimated parameters.[39] We next validated these predictions by performing the corresponding experiments. This experimental validation (Figure 5d, single data points) confirmed the model simulations thus demonstrating the predictive power of the quantitative model.

Following this comprehensive characterization of the green-light-responsive gene expression system in mammalian cells, we finally evaluated its suitability for controlling gene expression in plant cells. This would open the possibility of using optically induced gene expression in plant cells with reduced interference by endogenous plant photoreceptors primarily inducing signaling responses upon light in the UV-B, blue, and red parts of the spectrum.[16,17] For this purpose, we reengineered the constructs for use in plant backgrounds by cloning CarH-VP16 under the control of a constitutive CaMV35S promoter and by replacing SEAP by the firefly luciferase reporter. We transformed protoplasts isolated from *Arabidopsis thaliana* with the plasmid coding for CarH-VP16 and with reporter constructs harboring two, four, or eight CarO operator sites. After transformation, AdoB12 was added to a final concentration of 20 μM and cells were either illuminated for 24 h with 525 nm light (5 μmol m^{-2} s^{-1}) or kept in the dark. Assaying luciferase activity revealed increasing luminescence values with an increasing number of CarO operators (Figure 6). In alignment with the data obtained in mammalian cells, the reporter with eight CarO operator sites resulted in the highest absolute activity and fold-repression (ca. 16-fold) in response to 525 nm light illumination. These data demonstrate that the green light-responsive gene expression system is also functional in plant cells.

In this work, we describe the development and characterization of the first green-light-responsive gene expression system functional in mammalian and plant cells. The quantitative characterization of the systems performance using the mathematical model enables the *in silico*-based, rational design of expression profiles as demonstrated in the validation of the model predictions. This will strongly facilitate the application of this system for programming desired expression profiles. The green light-responsive-system requires the chromophore AdoB12. While potentially representing a limitation for future use in whole plants as they do not synthesize the cofactor, this dependence however is highly favorable in mammalian and plant cell culture as it enables the engineering of the biological system under ambient light while avoiding the inadvertent activation of CarH. The light-responsive properties can subsequently be conferred by the addition of AdoB12 that is readily taken up by mammalian and plant cells. The functionality of the system in plant protoplasts represents an important step toward the application of optogenetic systems in plant backgrounds. As plant photoreceptors are minimally responsive to green light, it is possible to achieve the orthogonal control of transgene activity with minimized cross-activation of endogenous light-responsive pathways. The synthetic switch based on CarH bridges the gap of wavelengths of use by adding green light to the existing systems in mammalian cells sensitive to UV-B, blue, red, and far-red light (see www.optobase.org)[13] and complements the red light-inducible gene expression switch in plant protoplasts previously reported[15,40] expanding the optogenetic toolbox for studies in plant cells. With these properties taken together, we believe that our expression system will foster advances in fundamental and application-oriented synthetic biology and optogenetics.

DOI: 10.1021/acssynbio.7b00450
ACS Synth. Biol. 2018, 7, 1349−1358

METHODS

DNA Cloning. The expression vectors were assembled by Gibson and AQUA[41] cloning. The resulting DNA sequences are indicated in Table 1.

Mammalian Cell Culture and Transfection. Human embryonic kidney cells (HEK-293, ATCC CRL-1573), human cervix carcinoma cells (HeLa, ATCC CCL-2), mouse fibroblasts (NIH-3T3, ATCC CRL-1658), and African green monkey fibroblast-like cells (COS-7, ATCC CRL-1651), were cultivated in DMEM-complete medium (Dulbecco's modified Eagle's medium (PAN, cat. no. P04-03550) supplemented with 10% fetal calf serum (FCS, PAN, cat. no. P30-3602, batch no. P101003TC) and 1% penicillin/streptomycin (PAN, cat. no. P06-07100)). Cells were transfected using a polyethylenimine (PEI)-based method as described before.[34] The expression vector encoding the activator CarH-VP16 (pHB144) was used in 4-fold excess (w:w) over the respective reporter plasmids (pCVC034/035/036). Unless indicated otherwise, after 24 h, the medium was replaced with fresh medium supplemented with 10 μM AdoB12 (Sigma, cat. no. C0884-10 mg). All experimental procedures after the addition of AdoB12 were carried out under safe red LED light (660 nm). After 1 h cultivation in the dark, the cells were illuminated with green LED light (525 nm; 5 μmol m^{-2} s^{-1}) unless indicated otherwise.

Protoplast Preparation and Transformation. Protoplast of *Arabidopis thaliana* were isolated from one to two-week old plantlet leaves (plants grown in a 23 °C, 16 h light−8 h dark regime) using the floatation method and the plasmids were transferred by polyethylene glycol-mediated transformation as described before.[42,40] Mixtures of the different plasmids as described in the figures to a final amount of 30 μg DNA (reporter plasmids pROF250/251/252 were added in a 3:1 molar ratio over the plasmid encoding CarH-VP16 pROF254) were used to transform 500 000 protoplasts in a final volume of 1.6 mL. After transformation, protoplasts were divided in aliquots of ca. 78 000 cells prior to the addition of AdoB12 to a final concentration of 20 μM, and subsequent illumination with green LED light (525 nm, 5 μmol m^{-2} s^{-1}) or incubation in dark for 24 h.

RNA Isolation and Real-Time Quantitative PCR Analysis. Cells were harvested at the indicated points in time and lysed for 5 min in 600 μL of peqGOLD TriFast (Peqlab/VWR, cat. no. 30-2010). Total RNA was isolated according to the manufacturer's instructions (Peqlab) and RNA integrity was validated by gel electrophoresis. Phenol/guanidin-isothiocyanat-based RNA isolation does not exclude plasmid DNA from the RNA fraction.[43] Accordingly, RNA samples of 5 μg were treated with DNase I for 30 min at room temperature, followed by purification with the RNA Clean & Concentrator kit (Zymo Research, R1013). cDNA was synthesized from 500 ng of total RNA using the First Strand cDNA Synthesis Kit (Thermo Fisher, K1612). To this end, total RNA was first mixed with both random hexamer and oligo $(dT)_{18}$-primers, incubated at 65 °C for 5 min and rapidly cooled to 4 °C. Synthesis of cDNA was conducted for 5 min at 25 °C, 60 min at 37 °C and terminated at 70 °C for 5 min. Quantitative PCR was performed directly with 0.5 μL of cDNA with the Absolute qPCR SYBR Green ROX Mix (Thermo Scientific, #AB-1162/B) in a total volume of 20 μL and in a qTOWER 2.0/2.2 device (Analytik Jena). For relative quantification of gene expression of SEAP, primers oNS092 (5′-CATGGACATTGACGTGATCCT-3′) and oNS093 (5′-CACCTTGGCTGTAGTCATCTG-3′) were used at final concentrations of 70 nM. For normalization, the reference gene beta-actin (ACTB) was amplified with the primers oNS100 (5′-CCCTGGAGAAGAGCTACGAG-3′) and oNS101 (5′-TCCATGCCCAGGAAGGAAG-3′). Each time-point was measured with three biological replicates in three repeats. Accumulation of the PCR-product was measured after every cycle for 40 cycles. The specificity of the amplification products was subsequently validated with both melting profiles and by gel electrophoresis. Furthermore, negative controls were included, in which the reverse transcriptase was omitted during cDNA synthesis to validate that residual plasmid DNA did not interfere with the sensitivity of the assay. C_q values were obtained with the qPCRsoft V3 software (Analytik Jena). PCR amplification efficiencies were determined as 100% with standard curves and relative expression levels were accordingly determined with the $\Delta\Delta C_q$ method.

Analytics. SEAP activity was determined in the cell culture medium using a colorimetric assay as described previously.[44] Firefly luciferase activity was determined in whole protoplasts as detailed elsewhere.[42,40] AdoB12 degradation was determined by seeding 0.3×10^6 HEK-293 cells mL^{-1} and adding 10 μM AdoB12. The decrease in AdoB12 concentration was followed by measuring the absorption spectrum of the cell medium every hour for 40 h. The AdoB12 concentration was calculated according to the height of its absorption peak at 525 nm, normalized with the absorption of medium lacking the cofactor.

ASSOCIATED CONTENT

Supporting Information

The Supporting Information is available free of charge on the ACS Publications website at DOI: 10.1021/acssynbio.7b00450.

Derivation of the mathematical model; measured and modeled dose−response characteristics and stability of AdoB12; identifiability analysis utilizing the parameter profile likelihood; fitted parameter values obtained by maximum likelihood estimation (PDF)

AUTHOR INFORMATION

Corresponding Authors

*E-mail: matias.zurbriggen@uni-duesseldorf.de.
*E-mail: wilfried.weber@bioss.uni-freiburg.de.

ORCID

Alex R. Jones: 0000-0001-6021-7824
Wilfried Weber: 0000-0003-4340-4446

Present Address

[▽]H.M.B.: Institute of Biotechnology, University of Helsinki, Finland.

Author Contributions

Conceptualization, M.Z., A.R.J., W.W.; methodology, C.V.C., R.O.F., R.E., N.S., H.B., J.T., M.Z., W.W.; investigation, C.V.C., R.O.F., R.E., N.S.; writing-original draft, C.V.C., R.O.F., R.E.; writing-review and editing, J.T., A.R.J., M.Z., W.W.; visualization, C.V.C., R.O.F., R.E.; supervision, J.T., M.Z., W.W.; funding acquisition, J.T., M.Z., W.W.

Notes

The authors declare no competing financial interest.

DOI: 10.1021/acssynbio.7b00450
ACS Synth. Biol. 2018, 7, 1349−1358

■ ACKNOWLEDGMENTS

We would like to thank Susanne Knall, Elke Wehinger, and Reinhild Wurm for their excellent technical assistance and Montserrat Elias-Arnanz for fruitful discussions. This work was supported by the Excellence Initiative of the German Federal and State Governments (BIOSS EXC-294, CEPLAS EXC-1028, SGBM GSC-4, and iGRAD-Plant GRK-1525) as well as by DFG grants to WW (WE 4733/4-1) and MZ (SPP1926 Z259/2-1).

■ REFERENCES

(1) Ausländer, S., and Fussenegger, M. (2013) From gene switches to mammalian designer cells : present and future prospects. *Trends Biotechnol. 31*, 155−168.
(2) Ausländer, S., Ausländer, D., and Fussenegger, M. (2017) Synthetic Biology — The Synthesis of Biology. *Angew. Chem., Int. Ed. 56*, 6396−6419.
(3) Baumgärtel, K., Genoux, D., Welzl, H., Tweedie-cullen, R. Y., Koshibu, K., Livingstone-zatchej, M., Mamie, C., and Mansuy, I. M. (2008) Control of the establishment of aversive memory by calcineurin and Zif268. *Nat. Neurosci. 11*, 572−578.
(4) Weber, W., Schoenmakers, R., Keller, B., Gitzinger, M., Grau, T., Sander, P., Fussenegger, M., and Daoud-El Baba, M. (2008) A synthetic mammalian gene circuit reveals antituberculosis compounds. *Proc. Natl. Acad. Sci. U. S. A. 105*, 9994−8.
(5) Ehrbar, M., Schoenmakers, R., Christen, E. H. E. H., Fussenegger, M., and Weber, W. (2008) Drug-sensing hydrogels for the inducible release of biopharmaceuticals. *Nat. Mater. 7*, 800−4.
(6) Xie, M., Ye, H., Wang, H., Charpin-El Hamri, G., Lormeau, C., Saxena, P., Stelling, J., and Fussenegger, M. (2016) Beta-cell-mimetic designer cells provide closed-loop glycemic control. *Science (Washington, DC, U. S.) 354*, 1296−1301.
(7) Kojima, R., Aubel, D., and Fussenegger, M. (2016) Toward a world of theranostic medication : Programming biological sentinel systems for therapeutic intervention. *Adv. Drug Delivery Rev. 105*, 66−76.
(8) Gossen, M., and Bujard, H. (1992) Tight control of gene expression in mammalian cells by tetracycline-responsive promoters. *Proc. Natl. Acad. Sci. U. S. A. 89*, 5547−51.
(9) Kramer, B. P., and Fussenegger, M. (2005) Hysteresis in a Synthetic Mammalian Gene Network. *Proc. Natl. Acad. Sci. U. S. A. 102*, 9517−9522.
(10) Fussenegger, M., Morris, R. P., Fux, C., Rimann, M., von Stockar, B., Thompson, C. J., and Bailey, J. E. (2000) Streptogramin-based gene regulation systems for mammalian cells. *Nat. Biotechnol. 18*, 1203−1208.
(11) Müller, K., Naumann, S., Weber, W., and Zurbriggen, M. D. M. D. (2015) Optogenetics for gene expression in mammalian cells. *Biol. Chem. 396*, 145−152.
(12) Weber, W., and Fussenegger, M. (2010) Synthetic gene networks in mammalian cells. *Curr. Opin. Biotechnol. 21*, 690−6.
(13) Kolar, K., and Weber, W. (2017) Synthetic biological approaches to optogenetically control cell signaling. *Curr. Opin. Biotechnol. 47*, 112−9.
(14) Olson, E. J., and Tabor, J. J. (2014) Optogenetic characterization methods overcome key challenges in synthetic and systems biology. *Nat. Chem. Biol. 10*, 502−511.
(15) Müller, K., Siegel, D., Rodriguez Jahnke, F., Gerrer, K., Wend, S., Decker, E. L., Reski, R., Weber, W., and Zurbriggen, M. D. (2014) A red light-controlled synthetic gene expression switch for plant systems. *Mol. BioSyst. 10*, 1679−88.
(16) Costa Galvão, V., and Fankhauser, C. (2015) Sensing the light environment in plants : photoreceptors and early signaling steps. *Curr. Opin. Neurobiol. 34*, 46−53.
(17) Kong, S. G., and Okajima, K. (2016) Diverse photoreceptors and light responses in plants. *J. Plant Res. 129*, 111−114.
(18) Wang, Y., and Folta, K. M. (2013) Contributions of green light to plant growth and development. *Am. J. Bot. 100*, 70−78.
(19) Ortiz-Guerrero, J. M., Polanco, M. C., Murillo, F. J., Padmanabhan, S., and Elías-Arnanz, M. (2011) Light-dependent gene regulation by a coenzyme B12-based photoreceptor. *Proc. Natl. Acad. Sci. U. S. A. 108*, 7565−7570.
(20) Jones, A. R. (2017) The photochemistry and photobiology of vitamin B $_{12}$. *Photochem. Photobiol. Sci. 16*, 820−834.
(21) Padmanabhan, S., Jost, M., Drennan, C. L., and Elías-Arnanz, M. (2017) A New Facet of Vitamin B $_{12}$: Gene Regulation by Cobalamin-Based Photoreceptors. *Annu. Rev. Biochem. 86*, 485−514.
(22) Jost, M., Fernández-Zapata, J., Polanco, M. C., Ortiz-Guerrero, J. M., Chen, P. Y., Kang, G., Padmanabhan, S., Elías-Arnanz, M., and Drennan, C. L. (2015) Structural basis for gene regulation by a B 12 -dependent photoreceptor. *Nature 526*, 536−541.
(23) Díez, A. I., Ortiz-Guerrero, J. M., Ortega, A., Elías-Arnanz, M., Padmanabhan, S., and Garcia de la Torre, J. (2013) Analytical ultracentrifugation studies of oligomerization and DNA-binding of TtCarH, a Thermus thermophilus coenzyme B12-based photosensory regulator. *Eur. Biophys. J. 42*, 463−476.
(24) Kainrath, S., Stadler, M., Reichhart, E., Distel, M., and Janovjak, H. (2017) Green-Light-Induced Inactivation of Receptor Signaling Using Cobalamin-Binding Domains. *Angew. Chem., Int. Ed. 56*, 4608−4611.
(25) Wang, R., Yang, Z., Luo, J., Hsing, I.-M., and Sun, F. (2017) B12-dependent photoresponsive protein hydrogels for controlled stem cell/protein release. *Proc. Natl. Acad. Sci. U. S. A. 114*, 5912−5917.
(26) Kutta, R. J., Hardman, S. J. O., Johannissen, L. O., Bellina, B., Messiha, H. L., Ortiz-Guerrero, J. M., Elías-Arnanz, M., Padmanabhan, S., Barran, P., Scrutton, N. S., and Jones, A. R. (2015) The photochemical mechanism of a B12-dependent photoreceptor protein. *Nat. Commun. 6*, 7907.
(27) Triezenberg, S. J., Kingsbury, R. C., and McKnight, S. L. (1988) Functional dissection of VP16, the trans-activator of herpes simplex virus immediate early gene expression. *Genes Dev. 2*, 718−729.
(28) Jacobsen, D. W., and Glushchenko, A. V. (2009) The transcobalamin receptor, redux. *Blood 113*, 3−4.
(29) Quadros, E. V., and Sequeira, J. M. (2013) Cellular uptake of cobalamin: Transcobalamin and the TCblR/CD320 receptor. *Biochimie 95*, 1008−1018.
(30) Weber, W., Fux, C., Daoud-el Baba, M., Keller, B., Weber, C. C., Kramer, B. P., Heinzen, C., Aubel, D., Bailey, J. E., and Fussenegger, M. (2002) Macrolide-based transgene control in mammalian cells and mice. *Nat. Biotechnol. 20*, 901−7.
(31) Rang, A., and Will, H. (2000) The tetracycline-responsive promoter contains functional interferon-inducible response elements. *Nucleic Acids Res. 28*, 1120−5.
(32) Verkhusha, V., Redchuk, T., Karasev, M., and Omelina, E. (2018) Near-infrared light-controlled gene expression and protein targeting in neurons and non-neuronal cells. *ChemBioChem*, DOI: 10.1002/cbic.201700642.
(33) Müller, K., Engesser, R., Metzger, S., Schulz, S., Kämpf, M. M. M., Busacker, M., Steinberg, T., Tomakidi, P., Ehrbar, M., Nagy, F., Timmer, J., Zubriggen, M. D. M. D., and Weber, W. (2013) A red/far-red light-responsive bi-stable toggle switch to control gene expression in mammalian cells. *Nucleic Acids Res. 41*, No. 377.
(34) Müller, K., Engesser, R., Schulz, S., Steinberg, T., Tomakidi, P., Weber, C. C. C., Ulm, R., Timmer, J., Zurbriggen, M. D. M. D., and Weber, W. (2013) Multi-chromatic control of mammalian gene expression and signaling. *Nucleic Acids Res. 41*, e124.
(35) Beyer, H. M. H. M., Juillot, S., Herbst, K., Samodelov, S. L. S. L., Müller, K., Schamel, W. W. W., Römer, W., Schäfer, E., Nagy, F., Strähle, U., Weber, W., and Zurbriggen, M. D. M. D. (2015) Red Light-Regulated Reversible Nuclear Localization of Proteins in Mammalian Cells and Zebrafish. *ACS Synth. Biol. 4*, 951−8.
(36) Levskaya, A., Weiner, O. D., Lim, W. A., and Voigt, C. A. (2009) sup: Spatiotemporal control of cell signalling using a light-switchable protein interaction. *Nature 461*, 997−1001.

DOI: 10.1021/acssynbio.7b00450
ACS Synth. Biol. 2018, 7, 1349−1358

(37) Raue, A., Kreutz, C., Maiwald, T., Bachmann, J., Schilling, M., Klingmüller, U., and Timmer, J. (2009) Structural and practical identifiability analysis of partially observed dynamical models by exploiting the profile likelihood. *Bioinformatics 25*, 1923−1929.
(38) Raue, A., Steiert, B., Schelker, M., Kreutz, C., Maiwald, T., Hass, H., Vanlier, J., Tönsing, C., Adlung, L., Engesser, R., Mader, W., Heinemann, T., Hasenauer, J., Schilling, M., Hofer, T., Klipp, E., Theis, F., Klingmüller, U., Schöberl, B., and Timmer, J. (2015) Data2-Dynamics: A modeling environment tailored to parameter estimation in dynamical systems. *Bioinformatics 31*, 3558−3560.
(39) Raue, A., Becker, V., Klingmüller, U., and Timmer, J. (2010) Identifiability and observability analysis for experimental design in nonlinear dynamical models. *Chaos 20*, 45105.
(40) Ochoa-Fernandez, R., Samodelov, S. L., Brandl, S. M., Wehinger, E., Müller, K., Weber, W., and Zurbriggen, M. D. (2016) Optogenetics in plants: Red/Far-red light control of gene expression, in *Optogenetics Methods and Protocols—Methods in Molecular Biology* (Kianianmomeni, A., Ed.) pp 125−139, Springer, New York.
(41) Beyer, H. M., Gonschorek, P., Samodelov, S. L., Meier, M., Weber, W., and Zurbriggen, M. D. (2015) AQUA cloning: A versatile and simple enzyme-free cloning approach. *PLoS One 10*, 1−20.
(42) Wend, S., Dal Bosco, C., Kämpf, M. M., Ren, F., Palme, K., Weber, W., Dovzhenko, A., and Zurbriggen, M. D. (2013) A quantitative ratiometric sensor for time-resolved analysis of auxin dynamics. *Sci. Rep. 3*, 2052.
(43) Rio, D. C., Ares, M. J., Hannon, G. J., and Nilsen, T. W. (2010) Removal of DNA from RNA. *Cold Spring Harb. Protoc. 2010*, 1−3.
(44) Schlatter, S., Rimann, M., Kelm, J., and Fussenegger, M. (2002) SAMY, a novel mammalian reporter gene derived from Bacillus stearothermophilus alpha-amylase. *Gene 282*, 19−31.

DOI: 10.1021/acssynbio.7b00450
ACS Synth. Biol. 2018, 7, 1349−1358